

SUPERCOMPUTER  
COMPUTATIONS  
RESEARCH INSTITUTE

NON-REVERSIBILITY OF MOLECULAR  
DYNAMICS TRAJECTORIES: WILL CHAOS  
DESTROY HMC?

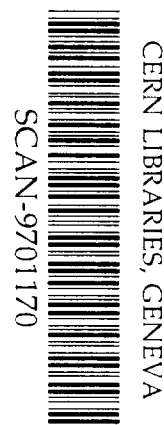
by

R.G. Edwards, I. Horváth, A.D. Kennedy

FSU-SCRI-96C-128

December 1996

THE FLORIDA STATE UNIVERSITY  
TALLAHASSEE, FLORIDA



SW9705

**IRREVERSIBILITY OF MOLECULAR DYNAMICS  
TRAJECTORIES:  
WILL CHAOS DESTROY HMC?**

R.G. EDWARDS, I. HORVÁTH, A.D. KENNEDY  
*Supercomputer Computations Research Institute, Florida State University,  
Tallahassee, FL 32303-4052, USA*

Hybrid Monte Carlo algorithm is the main computational tool used in the present-day simulations of full QCD. While its theoretical justification depends upon the molecular dynamics trajectories within it being exactly reversible, non-reversibility may arise due to amplification of rounding errors. We analyse the causes of such behaviour and give arguments, indicating that this probably does not pose a significant problem for Hybrid Monte Carlo computations. We present data for pure  $SU(3)$  gauge theory and for QCD with dynamical fermions on small lattices to illustrate and to support some of our ideas.

The theory of the Hybrid Monte Carlo (HMC) algorithm<sup>1,2</sup> assumes the exact reversibility of its molecular dynamics (MD) trajectories. Leapfrog integration guarantees this unless the initial conjugate gradient (CG) vector is chosen in time asymmetric way or finite precision arithmetic is used. While the first condition is easily ensured in practice by using a fixed starting vector for every CG inversion, all numerical computations carried out using floating point arithmetic are subject to rounding errors.

These rounding errors are normally not considered dangerous unless they are exponentially amplified. Indeed, without such an amplification, the time cost of reducing the error to some preset value grows only logarithmically with the number of arithmetic operations involved in the computation. This is a very small correction to the growth of the cost of the HMC algorithm as the volume and correlation length of the system are increased.

Exponential amplification will occur whenever nearby MD trajectories diverge from one another exponentially, i.e., when the MD evolution becomes unstable. There are two distinct mechanisms leading to such an instability<sup>3</sup>. First, this is typical for nonlinear equations in the chaotic regime. In fact, the existence of a positive leading Liapunov exponent for MD equations of pure  $SU(2)$  lattice gauge theory was recently suggested<sup>4</sup>. The second possibility is that the result of the discrete integration scheme diverges exponentially from the true solution. This instability should grow with the number of integration steps and is thus expected to have characteristic time scale shorter than the one associated with intrinsic chaos. Our numerical results confirm this.

The integration instability can be analysed in the context of free field

theory<sup>3</sup>, i.e. for the collection of independent modes with fixed frequencies. In fact, the behaviour of a single mode already reveals all the essential features. One can show that the instability accompanied by the exponentially decaying acceptance rate ( $P_{acc} \sim e^{-\nu\tau}$ ) occur when  $\omega\delta\tau \geq 2$ . Here  $\tau, \delta\tau$  and  $\omega$  are the trajectory length, the integration step size and the frequency of the mode respectively. In Fig. 1 the ' $\sigma = 0$ ' line shows the characteristic exponent  $\nu$  as a function of  $\delta\tau$  with  $\omega$  fixed to unity. Note the sharp "wall" arising at  $\delta\tau = 2$ , where the instability sets in.

Qualitatively similar behaviour is observed for the case of many stable modes<sup>3</sup>. The onset of instability is determined by the highest frequency mode and occurs when  $\omega_{max}\delta\tau = 2$ . In order to keep the acceptance rate constant for free field theory as the lattice volume  $V \rightarrow \infty$ , we must decrease  $\delta\tau$  so that  $V\delta\tau^4$  stays fixed. Consequently, the instabilities go away as we approach the thermodynamic limit. In this sense the leapfrog instability is a *finite volume effect*.

In interacting field theory the notion of independent modes loses its meaning. On the other hand, accepting the standard assumption that it can be still useful to think in these terms for asymptotically free field theories at short distances, it is quite plausible to expect similar scenario there too. The forces acting on the highest frequency mode due to the other modes will fluctuate in some complicated way however, and so we expect that the "wall" at  $\omega_{max}\delta\tau = 2$  will get smeared out. This is illustrated for the simple model of a harmonic oscillator whose frequency is randomly chosen from a Gaussian distribution with mean  $\omega$  and standard deviation  $\sigma$  before each MD step. The numerical results shown in Fig. 1 confirm that the "wall" in this model does indeed spread out.

Equipped with the above qualitative picture, we have studied reversibility numerically for  $SU(3)$  gauge theory both in the pure gauge and dynamical fermion cases<sup>3</sup> (see also related work<sup>5</sup>). We evolved a typical equilibrium configuration  $U$  using leapfrog equations for some time  $\tau$ , then reversed the momenta and evolved it again for the same amount of time to get the configuration  $U'$ . Deviations from reversibility were measured by

$$\|\Delta\delta U\|^2 \equiv \sum_{x,\mu} \sum_{a,b} |U_{x,\mu}^{a,b} - U'^{a,b}_{x,\mu}|^2, \quad (1)$$

where  $x, \mu$  and  $a, b$  are the space-time and  $SU(3)$  indices respectively. We also recorded the change of energy at the end of the trajectory ( $\delta H$ ) and at the end of the reversed trajectory ( $\Delta\delta H$ ).

In Fig. 2 we collected a typical set of data from one pure gauge configuration. The top and bottom graphs clearly show the integration instability

“wall” at  $\delta\tau \approx 0.6$ , which has spread out as expected. At the same time the middle graph indicates that as we reach the “wall”  $\delta H = O(10^3)$ , implying a negligible acceptance rate. The integration instabilities thus do not appear to have a practical importance for this system. Note however the case of the unreasonably long trajectory ( $\tau = 40$ ), where the reversibility is lost while  $\delta H$  is still very small.

When plotted as a function of  $\tau$ , all of our data show a clear exponential instability in  $\|\Delta\delta U\|$ . We extracted a characteristic exponent  $\nu$  ( $\|\Delta\delta U\| \sim e^{\nu\tau}$ ) and show the results in Fig. 3. Note the same qualitative behaviour we observed for the toy model in Fig. 1 except that the integration instability “wall” appears at different values of  $\delta\tau$ . This probably just reflects the different highest frequencies of these systems. In case of full QCD, the pseudofermions produce a force of the order of the inverse lightest fermionic mass thus giving the highest relevant frequency when simulating close to  $\kappa_c$ . This is reflected in the bottom graph where the integration instability appears at very small  $\delta\tau$ .

Notice also that the characteristic exponent does not approach zero for small  $\delta\tau$ , which confirms the existence of chaotic continuous time dynamics. Unlike the integration instability, the intrinsic chaos can not be controlled by adjusting  $\delta\tau$ . Moreover, accepting the standard hypothesis that the trajectory length should be scaled proportionally to the correlation length in order to reduce the critical slowing down, non-reversibility might cause problems when simulating closer to the continuum limit.

However, our numerical analysis indicates a strong  $\beta$ -dependence of the exponent  $\nu$ , characterizing the intrinsic chaos. Indeed, Fig. 4 shows this for  $SU(3)$  pure gauge theory on  $4^4$  and  $8^4$  lattices. These results can be qualitatively understood if we hypothesize that chaos is not only a property of this continuous time evolution, but is also a property of the underlying continuum field theory. This would suggest that  $\nu$  scales like a physical quantity. At small  $\beta$  the lattice theory is in the strong coupling regime and does not obey the asymptotic scaling behaviour. At large  $\beta$  the system is in a tiny box and is thus in the deconfined phase. The finite temperature phase transition at  $N_T = 4$  occurs near  $\beta = 5.7$ , suggesting that the scaling region is in the vicinity of this value for our lattices. We have fitted our  $8^4$  data at  $\beta = 5.4, 5.5, 5.6, 5.7$  to the one loop asymptotic scaling form  $\nu = ce^{-\beta/12\beta_0}$ , with  $\beta_0 = (11 - \frac{2}{3}n_f)/16\pi^2$  and with constant  $c$  being the only free parameter.

The resulting fit, shown in Fig. 4 is surprisingly good, suggesting that our hypothesis might indeed be correct. This might seem quite surprising at first, but one can gain some understanding of the mechanism by which chaos could weaken in the vicinity of the continuum limit by noting that  $\nu$  depends on  $\beta$  in two ways: there is an explicit  $\beta$ -dependence of the equations of motion,

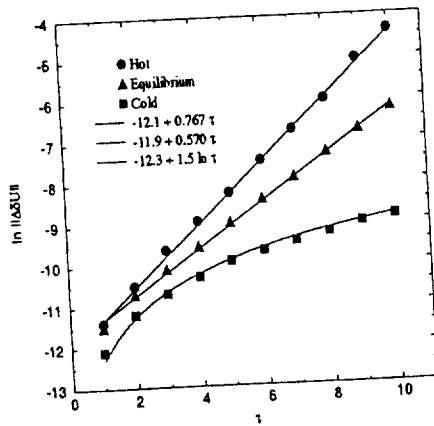


Figure 1:  $\ln \|\Delta\delta U\|$  is shown as a function of trajectory length for three starting gauge configurations at  $\beta = 5.1, \kappa = 0.16$ , and  $\delta\tau = 0.1$  on a  $4^4$  lattice.

and an implicit  $\beta$ -dependence in the equilibrium ensemble over which  $\nu$  is measured. The latter is illustrated in Fig. 5, where we plot  $\ln \|\Delta\delta U\|$  against  $\tau$  for three different configurations, one hot, one cold, and one chosen at random from the equilibrium distribution. The hot configuration yields the larger characteristic exponent than the equilibrium one, and the cold configuration is consistent with power law behaviour. Thus while  $\beta$  increases as we approach the continuum limit, the equilibrium ensemble increasingly prefers the ordered configurations over the disordered ones, reducing  $\nu$  as a result.

If our hypothesis is indeed correct, it would mean that the characteristic exponent is constant when measured in “physical” units, that is  $\nu\xi$  would be constant as  $\xi \rightarrow \infty$ . If this is the case, then tuning the HMC algorithm by varying the trajectory length proportionally to the correlation length does not lead to any change in the amplification of rounding errors as we simulate closer to the continuum limit.

#### Acknowledgments

This work was supported by the DOE under Grant Nos. DE-FG05-85ER250000 and DEFG05-92ER40742.

#### References

1. S. Duane, A.D. Kennedy, B.J. Pendleton and D. Roweth, *Phys. Rev. Lett.* **195B(2)**, 216 (1987).
2. P. de Forcrand, these proceedings; K. Jansen, these proceedings.
3. R.G. Edwards, I. Horváth and A.D. Kennedy, FSU-SCRI-96-49, hep-lat/9606004.
4. K. Jansen and C. Liu, *Nucl. Phys. B* **453**, 375 (1995).
5. K. Jansen and C. Liu, hep-lat/9607057.

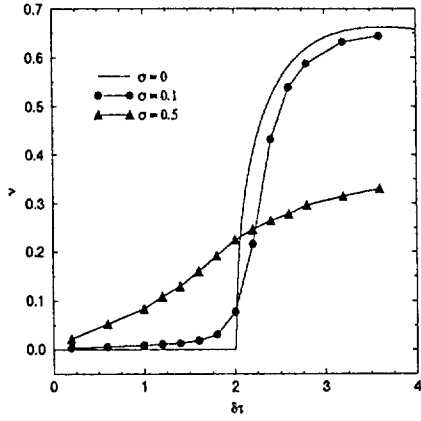


Figure 2: Characteristic exponent for the fluctuating-frequency harmonic oscillator model. The frequency fluctuates around  $\omega = 1$ .

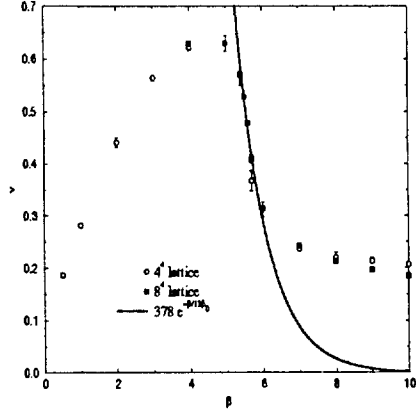


Figure 4: Characteristic exponent as a function of  $\beta$  for pure  $SU(3)$  gauge theory. The data was measured on three  $4^4$  and two  $8^4$  configurations.

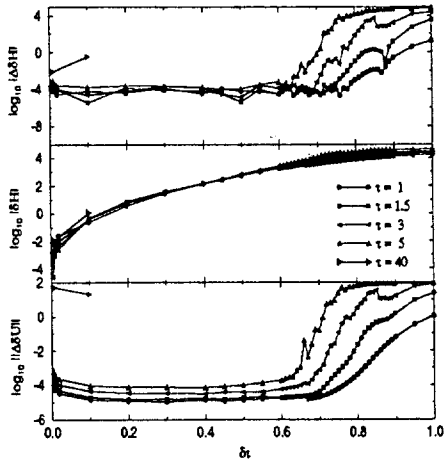


Figure 3: Results for pure  $SU(3)$  gauge theory with  $\beta = 5.7$  on a  $4^4$  lattice as a function of  $\delta\tau$ .

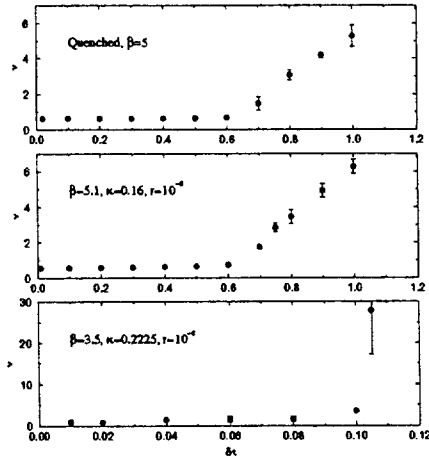


Figure 5: Characteristic exponent for pure  $SU(3)$  gauge theory (top), QCD with heavy dynamical Wilson quarks (middle), and QCD with light dynamical Wilson quarks (bottom). The data was measured on three independent configurations.

#### **DISCLAIMER**

This report was prepared as an account of work sponsored in part by an agency of the United States Government. Neither the United States Government nor any agency thereof, nor any of their employees, makes any warranty, express or implied, or assumes any legal liability or responsibility for the accuracy, completeness, or usefulness of any information, apparatus, product, or process disclosed, or represents that its use would not infringe privately owned rights. Reference herein to any specific commercial product, process, or service by trade name, trademark, manufacturer, or otherwise, does not necessarily constitute or imply its endorsement, recommendation, or favoring by the United States Government or any agency thereof. The views and opinions of authors expressed herein do not necessarily state or reflect those of the United States Government or any agency thereof.

This document is available upon request in alternate formats for individuals with print-related disabilities. Contact the Publications Department at (804) 644-1010 for more information.